

Ellipsometric Chain Length Dependence of Fatty Acid Langmuir Monolayers. A Heads-and-Tails Model

Jordan G. Petrov,* Thomas Pfohl, and Helmuth Möhwald

Max-Planck Institute of Colloids and Interfaces, Rudower Chaussee 5, 12489 Berlin, Germany

Received: November 11, 1998; In Final Form: February 10, 1999

Langmuir monolayers of even n -fatty acids with increasing number N of carbon atoms in the hydrocarbon chain ($N = 11$ – 23) were investigated on 1×10^{-2} M HCl aqueous subsolutions by means of Brewster angle ellipsometry. Isotherms, relating the coefficient of ellipticity $\Delta\rho$ to the area per molecule F , were continuously recorded and interpreted on the basis of literature phase diagrams and in situ X-ray reflectivity and diffraction investigations. $\Delta\rho/N$ dependencies for the liquid-expanded (LE), super-liquid or solid (LS/S), and condensed-solid (CS) monolayer phases were extracted from the isotherms at constant areas per molecule: $F_{LE} = 28 \pm 1 \text{ Å}^2$, $F_{LS/S} = 19.2 \pm 0.3 \text{ Å}^2$, $F_{CS} = 18.5 \pm 0.3 \text{ Å}^2$. They show $\Delta\rho$ -discontinuities at the LE–LS and S–CS transitions but no change at the LS–S transition. The experimental $\Delta\rho/N$ data for the solid condensed monolayer were compared with calculated $\Delta\rho/N$ dependencies using the “one-layer” ellipsometric model with bulk isotropic or theoretical anisotropic n/N data. A very good agreement of $d\Delta\rho_{\text{exp}}/dN$ with the slope of the calculated “isotropic” dependence, and a significant difference from the “anisotropic” slope was observed. The calculated “isotropic” $\Delta\rho/N$ dependence was shifted to higher $\Delta\rho$ -values probably due to a different hydration state of the carboxyl groups in the bulk solid phase and Langmuir monolayer. The “one-layer” model was also used in the alternative calculation of the isotropic refractive indices of the LE, LS–S, and CS phases from our $\Delta\rho/N$ data. The obtained n/N dependencies were compared with bulk n/N data for n -fatty acids and n -alkanes which differ only by a terminal COOH group. No agreement was found between bulk and monolayer values. A similarity of the trends was observed for the RCOOH system; both the bulk and monolayer n/N dependencies show discontinuities at the liquid–solid, as well as the LE–LS, phase transition. In contrast, the n/N dependence of the bulk n -alkanes is smooth for N between 5 and 30. Such a behavior shows that the headgroups contribute specifically to the optical characteristics of Langmuir monolayers. A simple “heads-and-tails” model based on the Lorentz–Lorentz relationship was proposed to relate the ellipsometric signal of the monolayer to the polarizability and thickness of the headgroup and hydrocarbon chain regions and to the optical anisotropy of the latter. Application of this model to our $\Delta\rho/N$ data under some physical restrictions shows that the anisotropy of the methyl group in closely packed vertical chains is below 3.3% of the isotropic value. The ellipsometric dimension of the monolayer headgroups obtained implies that they have hydration shells approximately one water molecule thick. The model explains the observation reported in the literature¹⁰ that Cd^{2+} and Pb^{2+} dissolved in the water substrate shift the ellipsometric chain length dependence to higher $\Delta\rho$ -values without affecting its slope. This effect seems to be due to the increased polarizability and decreased thickness (partial dehydration) of the headgroup region resulting from Cd^{2+} and Pb^{2+} binding to the carboxyl groups.

Introduction

Ellipsometry has been often applied to determine the optical constants and thickness of thin organic films on solid and liquid substrates. The interpretation of the data was usually based on the “one-layer” model, which ascribes a uniform refractive index, n , and an ellipsometric thickness, d , to the film. For thicker films both quantities can be determined simultaneously, but for monolayers at the air–water interface or adsorbed (self-assembled) monolayers on solid substrates such a determination is impossible.^{1,2} Molecular models, X-ray reflectivity data, or an a priori assumption that the substance retains its bulk density in monolayer state are used to estimate d and to calculate n .^{3,4,5} When the thickness has to be obtained, an appropriate value of n has to be introduced in the “one-layer” ellipsometric equation.

Most of the studies neglect the dependence of the monolayer refractive index on d pragmatically motivated by the estimation^{6–8} that a 0.05 units variation of n changes the thickness by less than 1 Å. For example, Allara and Nuzzo⁶ used the bulk refractive index of $\text{C}_{21}\text{H}_{43}\text{COOH}$ to calculate the thicknesses of the adsorption layers of C6–C24 n -fatty acids on oxidized aluminum and Wasserman et al.⁷ estimated the thicknesses of C10–C18 alkylsiloxane monolayers on silicone employing the refractive index of bulk paraffins.

However, Hofmester⁵ found that the bulk refractive indices of the solid n -fatty acids significantly exceed the monolayer values for the same substances estimated from the “one-layer” model. Den Engelsen and de Koning⁹ attributed this difference to an optical anisotropy of the condensed monolayer, where the hydrocarbon chains are closely packed and parallel to each other. An alternative explanation could be the ellipsometric contribution of the monolayer headgroups and hydration water. Some authors assume that because of their hydration the headgroups

* Corresponding author. On leave of absence from Institute of Biophysics, Bulgarian Academy of Sciences, 1 Acad. G. Bonchev St., Block 21, 1113 Sofia, Bulgaria

are optically indistinguishable from the water substrate;^{3,4,11} others¹² include their dimension in the thickness but do not consider their contribution to the monolayer refractive index. Explicit treatment of this problem implies distinguishing between the ellipsometric contributions of the heads and the tails, and here we propose a simple version of such a “heads-and-tails” model.

An investigation of the chain length dependence of the ellipsometric signal introduces a new variable, the number of carbon atoms in the chain N , and yields additional information from the slope of this dependence if it is linear. Previous studies of fatty acid Langmuir monolayers showed that this is indeed the case. Den Engelsen and de Koning⁹ studied the even C14–C22 homologues on 1×10^{-3} M HCl and found a linear increase of the change of the ellipsometric phase angle, $\delta\Delta$, with N , and Kim et al.¹⁰ obtained a linear $\delta\Delta/N$ relationship for monolayers of C15, C16, C18, and C22 n -fatty acids on 1×10^{-2} M HCl. Linear dependencies with the same slope, specifically shifted along the ordinate, were found in ref 10 when subsolutions containing CdCl_2 or PbCl_2 were used instead of 1×10^{-2} M HCl. Cd^{2+} and Pb^{2+} bind specifically to the carboxylic groups,^{13,14} and one could expect specific changes of their polarizability and hydration, which modify the refractive index and dimensions of that monolayer region. The “one-layer-model” implicitly accounts for this effect when the bulk refractive index of the corresponding soap is utilized, but a more detailed “heads-and-tails” model distinguishing the contribution of the polar heads and the hydrocarbon chains would treat the problem more explicitly.

Unfortunately the above-mentioned ellipsometric chain-length dependencies^{5,9,10} were registered at different areas per molecule, F , and do not correspond to the same monolayer phase. This fact might be important, because the conformation of the hydrocarbon chains, their tilt angle, the hydration, and dimension of the headgroups, vary with the area per molecule^{15,16} and these changes are sensed by the ellipsometric isotherms (see the Experimental Section of this study). When F varies one cannot distinguish the chain length effect from the effect of density on monolayer refractive index. This study pays a special attention to this problem. We continuously record the $\Delta\rho/F$ -isotherms of even C12–C24 n -fatty acids measuring the coefficient of ellipticity $\Delta\rho$ via Brewster angle ellipsometry. The monolayer phases are identified from the changes of the slope of the isotherms, from phase diagrams¹⁷ and in situ X-ray reflectivity and diffraction data.^{18–20} $\Delta\rho/N$ -dependencies at fixed areas per molecule corresponding to the liquid-expanded (LE), super-liquid or solid (LS/S), and condensed-solid (CS) phases are extracted from the isotherms. The mean refractive indices for these phases are calculated applying the “one-layer” model, and the monolayer n/N dependencies thus obtained are compared with n/N data for fatty acids and alkanes in liquid and solid bulk state. The comparison shows that the COOH groups specifically contribute to both the monolayer and bulk n/N dependencies, which qualitatively differ from the bulk n/N data for the alkanes.

A simple two-layers “heads-and-tails” model utilizing the Lorentz–Lorentz relationship is proposed to account for this contribution. It relates the ellipsometric signal of the monolayer to the polarizability and thickness of the headgroups and hydrocarbon chains and to the optical anisotropy of the latter. Application of this model to our $\Delta\rho/N$ dependence for the solid condensed monolayer ($F = 19.3 \pm 0.5 \text{ \AA}^2$) shows that in this state the anisotropy of the methyl group is below 3.3% of the isotropic value. The monolayer headgroups have hydration shells

about one water molecule thick. The model explains the observation,¹⁰ that addition of Cd^{2+} and Pb^{2+} in the aqueous substrate causes specific shifts of the ellipsometric chain length dependence of fatty acid monolayers to higher $\Delta\rho$ -values. This effect seems to be due to increased polarizability and decreased thickness (partial dehydration) of the headgroups region, resulting from the counterion binding to the carboxyl groups.

Theoretical Background

One-Layer Model of the Chain Length Dependence of the Ellipsometric Signal: Ellipsometry determines the complex ratio r of the p and s amplitudes r_p and r_s of the light reflected from an interface:

$$r = \frac{r_p}{r_s} = \text{Re}(r) + i\text{Im}(r) = \rho e^{i\Delta} \quad (1)$$

A Langmuir monolayer changes the value of r for the pure water surface. For nonabsorbing amphiphilic substances the measurement of r at the Brewster angle gives $\text{Re}(r) = 0$ and $\rho = \text{Im}(r)$. This quantity, known as coefficient of ellipticity, is related to the refractive indices of air, n_1 , water, n_2 , and monolayer, n , by the formula

$$\rho = \frac{\pi}{\lambda} \frac{\sqrt{n_1^2 + n_2^2}}{n_1^2 - n_2^2} \eta \quad (2)$$

For a monolayer exhibiting an uniaxial anisotropy in direction z perpendicular to the surface, $n_z \neq n_x = n_y$, and η reads

$$\eta = \int_{-\infty}^{\infty} \left(n_x^2 - n_1^2 - n_2^2 + \frac{n_1^2 n_z^2}{n_z^2} \right) dz \quad (3)$$

The case $n_z = n_x = n$ corresponds to an isotropic monolayer. The same relationship holds for the change of the coefficient of ellipticity $\Delta\rho = \rho - \rho_0$, where ρ_0 refers to the pure air–water interface.

The “one-layer” model postulates an abrupt change of the dielectric properties at the air–monolayer and monolayer–water boundaries and an uniform refractive index of the space between them having thickness d . These simplifications modify eq 3 to give

$$\Delta\rho = \frac{\pi}{\lambda} \frac{\sqrt{n_1^2 + n_2^2}}{n_1^2 - n_2^2} \left(n_x^2 - n_1^2 - n_2^2 + \frac{n_1^2 n_z^2}{n_z^2} \right) d \quad (4)$$

Differentiating eq 4 with respect to N at constant monolayer density and substituting dd/dN by the contribution of a CH_2 group d_{CH_2} to the thickness one obtains

$$\frac{d\Delta\rho}{dN} = \frac{\pi}{\lambda} \frac{\sqrt{n_1^2 + n_2^2}}{n_1^2 - n_2^2} \left[\left(\frac{dn_x^2}{dN} - \frac{n_1^2 n_2^2}{n_z^4} \frac{dn_z^2}{dN} \right) d + \left(n_x^2 - n_1^2 - n_2^2 + \frac{n_1^2 n_z^2}{n_z^2} \right) d_{\text{CH}_2} \right] \quad (5)$$

If the monolayer refractive index does not depend on N and the area per molecule is fixed, the first term in the square

brackets disappears and we obtain

$$\frac{d\Delta\rho}{dN} = \frac{\pi}{\lambda} \frac{\sqrt{n_1^2 + n_2^2}}{n_1^2 - n_2^2} \left(n_x^2 - n_1^2 - n_2^2 + \frac{n_1^2 n_2^2}{n_z^2} \right) d_{\text{CH}_2} = \text{const} \quad (6)$$

Equation 6 shows that at constant d_{CH_2} (fixed F) the $\Delta\rho/N$ dependence should be linear if the mean refractive index of the monolayer, isotropic or anisotropic, does not depend on chain length. Therefore, if it indeed would be the case, one would be able to rather accurately calculate the mean isotropic refractive index n without knowing the total monolayer thickness just introducing in eq 6 the experimental slope $d\Delta\rho/dN$ and the well-established value of d_{CH_2} .

“Heads-and-Tails” Model of the $\Delta\rho/N$ Dependence. The dependence of the monolayer refractive index on the number of carbon atoms in the hydrocarbon chain can be obtained from the Lorentz–Lorentz relationship

$$\frac{n^2 - 1}{n^2 + 2} = \frac{4\pi}{3} \frac{\alpha}{v} \quad (7)$$

assuming independent contributions of the hydrophilic heads, methylene and methyl groups to the molecular polarizability α , and molecular volume v . If the polarizability along the chain is α_{\parallel} , the one perpendicular to it is α_{\perp} , and if the monolayer molecules are inclined at an angle Θ from the normal to the interface, the components of α along x and z axis can be written as

$$\alpha_x = \frac{(\alpha_{\perp} + \alpha_{\perp} \cos\Theta + \alpha_{\parallel} \sin\Theta)}{2} \quad (8a)$$

$$\alpha_z = \alpha_{\parallel} \cos\Theta + \alpha_{\perp} \sin\Theta \quad (8b)$$

Neglecting the difference between the CH_2 and CH_3 groups and assuming that the optical anisotropy of the monolayer is due to an anisotropy of the methylene groups, we can present α_{\perp} and α_{\parallel} as

$$\alpha_{\perp} = \alpha_0 + N\alpha_{\perp, \text{CH}_2} \quad (9a)$$

$$\alpha_{\parallel} = \alpha_0 + N\alpha_{\parallel, \text{CH}_2} \quad (9b)$$

Here α_0 is the isotropic headgroup polarizability, and $\alpha_{\perp, \text{CH}_2}$ and $\alpha_{\parallel, \text{CH}_2}$ are the anisotropic methylene group polarizabilities, respectively, perpendicular and parallel to the chain. The molecular volume can be related to the area per molecule F , and dimensions of the head d_0 , and the CH_2 group, d_{CH_2} , along the chain

$$v = F(d_0 + Nd_{\text{CH}_2})\cos\Theta \quad (10)$$

Introducing eqs 8–10 in eq 7 we obtain the dependence of the anisotropic refractive indices n_x and n_z on N . Equations 4 and 7–10 give the dependence of the ellipsometric signal $\Delta\rho$ on the number of carbon atoms in the hydrocarbon chain N .

Numerical simulations with eqs 4 and 7–10 for a solid condensed monolayer with a tilt angle $\Theta = 0^\circ$ show that (i) A positive anisotropy of polarizability of the methylene group, $\alpha_{\parallel, \text{CH}_2} > \alpha_{\perp, \text{CH}_2}$, and monolayer molecules, $\alpha_{\parallel} > \alpha_{\perp}$, resulting in positive refractive index anisotropy, $n_{\parallel} > n_{\perp}$, reduces the slope of the $\Delta\rho/N$ dependence compared to the isotropic case. (ii) The slope of the isotropic $\Delta\rho/N$ dependence increases if the molecular polarizability, as well as the refractive index, is increased. (iii) Increasing the headgroup polarizability α_0 at

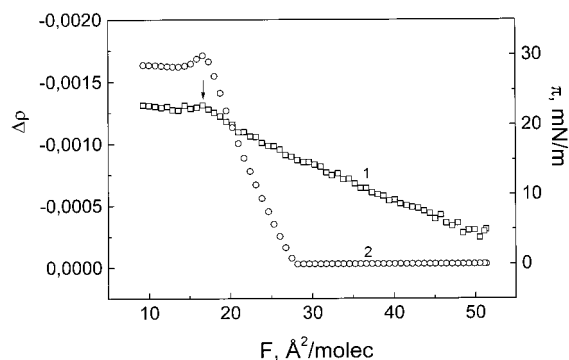


Figure 1. Ellipsometric isotherm, $\Delta\rho/F$, (curve 1), and surface pressure isotherm, π/F (curve 2), of lauric acid on an aqueous subsolution of 1×10^{-2} M HCl. The arrow indicates the collapse point whose ordinate does not depend on the compression rate. The abscissa values are not representative because of the slight solubility of this acid.

constant Z -dimension d_0 , increases the values of $\Delta\rho$, but does not change the slope $d\Delta\rho/dN$. (iv) Increasing the Z -dimension of the headgroup d_0 at fixed α_0 decreases the values of $\Delta\rho$ retaining the same slope $d\Delta\rho/dN$.

Experimental Section

Materials and Methods. The Fluka fatty acids of 99+ % purity were used as received. The monolayers were spread as 1mM chloroform solutions on 1×10^{-2} M HCl aqueous substrates. The latter were prepared with Millipore Milli-Q water and HCl of AR grade of purity.

Continuous and simultaneous measurements of the coefficient of ellipticity ρ and surface pressure π were performed in a rectangular Teflon trough of a Langmuir balance. A Wilhelmy type dynamometric system using a strip of filter paper for good wettability registered surface pressure. A birefringence modulation ellipsometer²¹ operated at the Brewster angle of beam incidence and fixed wavelength $\lambda = 632.8$ nm was applied for determination of ρ . The area illuminated by the laser beam was 1 mm². After spreading of the chloroform solution on the water surface, 2 min were left for evaporation of the solvent and the monolayers (except for the lauric acid) were compressed at a speed of 2 Å²/molecule min. The temperature of the water substrate was kept constant at 22 °C by a thermostat.

Ellipsometric Isotherms and Phase transitions in the Monolayer. In this section we describe our $\Delta\rho/F$ and π/F isotherms and analyze them using literature phase diagrams and X-ray reflectivity and diffraction data to identify monolayer phases as a function of monolayer density. Four characteristic isotherms are chosen as representative in Figures 1–4. The $\Delta\rho/F$ dependencies of myristic and arachidic acids shown in Figures 2 and 3 are in a good agreement with the $\delta\Delta/F$ isotherms of the same substances reported by den Engelsen and de Koning,⁹ but the higher sensitivity of the Brewster angle ellipsometry and the continuous recording of $\Delta\rho$ during compression used in this study visualized some phase transitions which were not detected previously.

Lauric Acid. The ellipsometric isotherm (curve 1, Figure 1) shows that $\Delta\rho$ smoothly increases with decreasing F without any changes of the slope which would indicate phase transitions. It exhibits a small convex curvature toward the abscissa achieving a maximum value at the collapse point (see the arrow) and asymptotically tending to $\Delta\rho = 0$ at large areas per molecule. The values on the abscissa are not representative because of the slight solubility of this acid. However, the investigation of the desorption rate of decanoic acid²² gives a

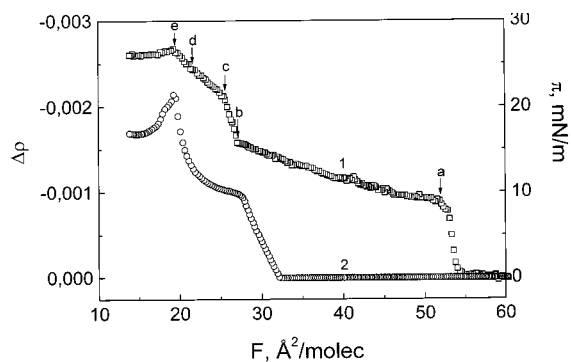


Figure 2. Ellipsometric isotherm, $\Delta\rho/F$ (curve 1), and surface pressure isotherm, π/F (curve 2), of myristic acid on 1×10^{-2} M HCl. The arrows indicate transformations of the monolayer structure: see the text.

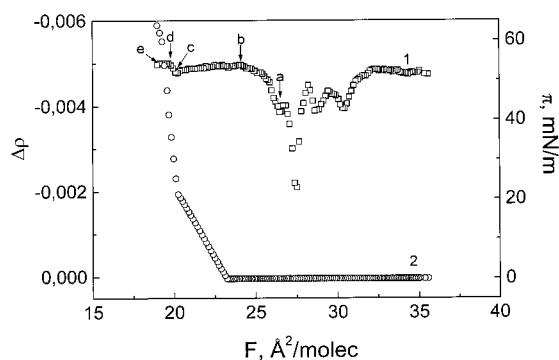


Figure 3. Ellipsometric isotherm, $\Delta\rho/F$ (curve 1), and surface pressure isotherm, π/F (curve 2), of arachidic acid on 1×10^{-2} M HCl. The arrows show changes of the monolayer structure.

minimum area of 28.6 \AA^2 per molecule and we expect the collapse area of the lauric acid to be close to this value. The collapse values of $\Delta\rho$ are characteristic and remain the same after a 3-fold increase of the compression speed.

Myristic Acid. Curve 1 in Figure 2 shows the ellipsometric isotherm of the myristic acid. The changes of the slope are marked by arrows and the sections between them are analyzed according to the phase diagram of Bibo and Pitsersen.¹⁷ The liquid-expanded part a–b between 52 and 27 \AA^2 strongly resembles the $\Delta\rho/F$ isotherm of the lauric acid, but the maximum LE-value of $\Delta\rho$ is higher. In this region of disordered (liquid) hydrocarbon chains the coefficient of ellipticity increases due to increasing density, respectively the refractive index, and may be increasing thickness of the monolayer. In the intermediate b–c region (27 – 25 \AA^2), the LE and the liquid-condensed L2 phases coexist and $\Delta\rho$ steeply rises because of the increasing portion of the denser and thicker L2 phase. In the c–d region (25 – 21 \AA^2), where the monolayer is in the L2 phase, $\Delta\rho$ increases because of the gradual transition of the monolayer molecules from a tilted ($\Theta = 23$ – 30°) to upright position.^{15,18} A super-liquid (LS) phase of vertical molecules which are free to rotate exists in the d–e region^{15–18} between 21 \AA^2 and the collapse area of 19.2 \AA^2 . The increase of $\Delta\rho$ in this part of the isotherm occurs at constant monolayer thickness and slightly increasing density. One might speculate that a progressive dehydration of the headgroups decreases the dimension and increases the polarizability of that monolayer region ($\alpha_{\text{H}_2\text{O}} = 1.5 \text{ \AA}^3$, $\alpha_{\text{COOH}} = 3.3 \text{ \AA}^3$). According to the predictions of the “heads-and-tails” model both effects increase $\Delta\rho$.

Arachidic Acid. Figure 3 shows the $\Delta\rho/F$ and π/F isotherms of arachidic acid which are typical for the fatty acids from $\text{C}_{15}\text{H}_{31}\text{COOH}$ to $\text{C}_{19}\text{H}_{39}\text{COOH}$. Fluctuations of the ellipsometric

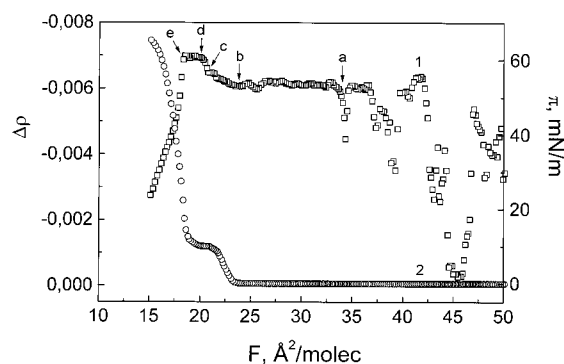


Figure 4. Ellipsometric isotherm, $\Delta\rho/F$ (curve 1), and surface pressure isotherm, π/F (curve 2), of tetracosanoic acid on 1×10^{-2} M HCl. Structural changes of the monolayer are indicated by arrows: see explanation in the text.

signal, indicating islands of a condensed monolayer with characteristic high values of $\Delta\rho$, are observed above 27 \AA^2 . A strong increase of the ellipsometric signal can be seen in the region a–b between 27 and 24 \AA^2 where the transition to a continuous monolayer in L2 phase occurs. In the L2 region b–c between 24 and 20.4 \AA^2 $\Delta\rho$ slightly decreases and passes through a minimum at the L2–LS transition occurring at 20.4 \AA^2 . The reason for such a decrease is unclear so far. The X-ray reflectivity data¹⁸ show that in the b–c part of the isotherm the total thickness of the monolayer increases because the transition from tilted to vertical chains overcompensates the decrease of the headgroups dimension which is probably due to their (partial) dehydration. In the LS region c–d between 20.4 and 19.8 \AA^2 , $\Delta\rho$ increases at constant thickness because of increasing density and further headgroups dehydration. This process seems to be completed at 19.8 \AA^2 , and $\Delta\rho$ remains constant in the S-phase d–e region down to the collapse area of 19.0 \AA^2 .

Tetracosanoic Acid. The phase transitions of this monolayer have been studied via GIXD and specular reflection by Schlossman et al.²⁰ This study and the X-ray diffraction investigation of behenic acid¹⁹ were used for interpretation of the ellipsometric isotherm (curve 1, Figure 4). The strong fluctuations above 35 \AA^2 with minimum values of $\Delta\rho = 0$ and maximum $\Delta\rho$ values corresponding to the condensed phase support the previous observation²⁰ that 2D crystalline domains, which coexist with a gaseous monolayer, are formed just after spreading of this acid. In the region a–b between 35 and 23.5 \AA^2 these domains are being packed progressively denser. The GIXD study shows that they exhibit two characteristic peaks of a distorted hexagonal (rectangular) phase, with an unit cell area of 22.3 \AA^2 and a tilt angle $\Theta = 30^\circ$. From 23.5 to 20.7 \AA^2 in the b–c region, $\Delta\rho$ increases due to decreasing of the tilt angle from 30° to 15° in the L2 phase. In the c–d region between 20.7 and 19.3 \AA^2 , the increase of $\Delta\rho$ is steeper because of the further decrease of Θ from 15° to 0° and transition to a denser rectangular S phase with an unit cell area of 19.4 \AA^2 . Between 19.3 \AA^2 and the collapse area of 18.3 \AA^2 (in the d–e region), where the ellipsometric signal remains constant, the GIXD investigation²⁰ shows a single untilted CS-phase with an unit cell area of 18.5 \AA^2 .

Chain-Length Dependence of the Ellipsometric Signal in the LE, LS or S, and CS Phases. Figure 5 shows the $\Delta\rho/N$ dependence for the LE, LS/S (LS or S), and CS phases extracted from the $\Delta\rho/F$ isotherms at the corresponding characteristic areas per molecule, $F_{\text{LE}} = 28 \pm 1 \text{ \AA}^2$, $F_{\text{LS/S}} = 19.2 \pm 0.3 \text{ \AA}^2$, and $F_{\text{CS}} = 18.5 \pm 0.3 \text{ \AA}^2$. They include the collapse value of the lauric acid, the maximum LE-value at 27 \AA^2 and the LS (collapse) value at 19.2 \AA^2 of the myristic acid, the plateau

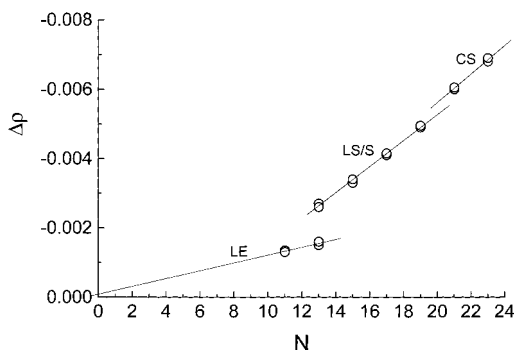


Figure 5. Dependence of the ellipsometric signal $\Delta\rho$ on the number of carbon atoms N in the hydrocarbon chain for the LE, LS/S, and CS phases. The data are extracted from the isotherms at the corresponding area per molecule, $F_{LE} = 28 \pm 1 \text{ \AA}^2$, $F_{LS/S} = 19.2 \pm 0.3 \text{ \AA}^2$, $F_{CS} = 18.5 \pm 0.3 \text{ \AA}^2$.

values before collapse for the palmitic and stearic acids which correspond to the LS phase, the value of the S phase in the d-e plateau of the arachidic acid, and the plateau values for behenic and tetracosanoic referring to the CS phase. The LE and the CS parts are represented by only two homologues each, but several measurements with a good reproducibility confirm these data.

The LE–LS and S–CS phase transitions are clearly indicated as $\Delta\rho$ -discontinuities, but no LS–S transition can be distinguished. The larger change of $\Delta\rho$ at the LE–LS transition is probably due to the simultaneous increase of the density, respectively of the refractive index, and the thickness of the monolayer, which accompany the transition from disordered to vertically oriented and closely packed chains. At the S–CS transition, the monolayer density changes only slightly and the vertical orientation of the molecules remains the same. Nevertheless, the values of $\Delta\rho$ in the CS phase are higher than those expected from the extrapolation of the S-part of the $\Delta\rho/N$ dependence. This might come from an effective increase of the monolayer thickness due to a “staggered” structure appearing before collapse where some of the molecules are shifted up- and downward.²³ The resulting roughness of the monolayer–air interface might also contribute to the increase of the ellipsometric signal.²

It is interesting that the linear extrapolation of the LE part passes the origin of the coordinate system (the intercept is statistically insignificant). If such an extrapolation is correct, this means that the contribution of the hydrophilic heads to the coefficient of ellipticity is negligible in the LE phase. Such a conclusion seems plausible because of the complete hydration of the headgroups in this monolayer state. The linearity of the LE section finds support from the X-ray diffraction investigation of Wolgast, Förster, and Brezesinski²⁴ on the liquid-crystalline L_α phase of hydrated 1,2-diols in which the hydrocarbon chains are also fluid. These authors register a linear increase of the periodical interlamellar distance with chain length and estimate the dimension of the water core via extrapolation to zero length of the chain.

The LE part of the $\Delta\rho/N$ dependence shows also that the physically unreasonable positive intercepts of the $\delta\Delta/N$ dependencies discussed in the literature¹⁰ result from neglecting the LE–LS phase transition. Such intercepts were obtained via extrapolation to $N = 0$ of the $\delta\Delta/N$ data for closely packed and vertically oriented molecules ignoring the fact that the solid condensed monolayer structure does not exist at small values of N where the van der Waals attraction between the chains is insufficient to prevent their thermal disorder.

Application of the “One-Layer” Model to our $\Delta\rho/N$ Data. $\Delta\rho/N$ Dependence of the Solid Condensed Monolayer. The

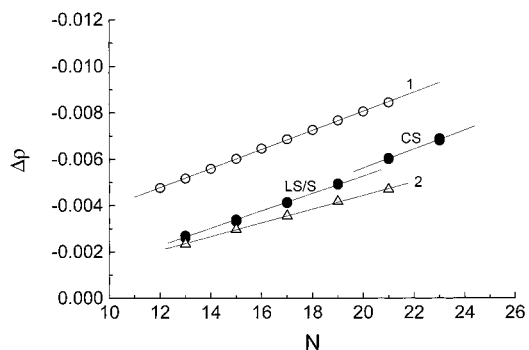


Figure 6. Comparison of the experimental $\Delta\rho/N$ data with the “isotropic” dependence (curve 1) calculated from eqs 4 and 11 with the bulk refractive indices of the fatty acids⁵ and the “anisotropic” dependence (curve 2) obtained from eqs 4 and 11 with the values of n_x and n_z reported by den Engelsen.¹²

LS/S part of the $\Delta\rho/N$ dependence obeys a linear fit with a correlation coefficient $R = 0.9984$ and a standard deviation of the fit $SD = 5.6 \times 10^{-5}$. The observed linearity might imply an independence of the monolayer refractive index on N and validity of eq 6. In such a case one would be able to determine the mean isotropic refractive index of the LS/S phase from the slope $d\Delta\rho/dN$ and the value of $d_{CH_2} = 1.27 \text{ \AA}$. However, the observed behavior proves to be deceptive since even when n and d vary with N one obtains good straight lines. Figure 6 illustrates this fact presenting the $\Delta\rho/N$ dependencies calculated from the complete eq 4 with experimental n/N data from ref 5 for isotropic bulk refractive indices of solid fatty acids (curve 1) and anisotropic refractive indices theoretically estimated by den Engelsen¹² (curve 2). In both calculations the monolayer thickness was evaluated from the precise length of the all-trans molecular configuration

$$d = d_0 + (N-1)d_{CH_2} + d_{CH_3} \quad (11)$$

with X-ray data¹⁸ for $d_0 = 3.1 \text{ \AA}$, $d_{CH_2} = 1.27 \text{ \AA}$, and $d_{CH_3} = 1.42 \text{ \AA}$. The dependencies thus obtained take into account both the variation of the refractive index and the thickness of the monolayer with N , but represent excellent straight lines with $R_{(1)} = 0.9998$ and $R_{(2)} = 0.9996$. Therefore, the constant value of $d\Delta\rho/dN$ does not prove the independence of the monolayer refractive index on N and the validity of eq 6.

The slope of the “isotropic” curve 1, $(4.1 \pm 0.05) \times 10^4$, practically coincides with the slopes of our “monolayer” dependencies in the LS/S state, $(3.8 \pm 0.1) \times 10^4$, and the CS state, $(4.1 \pm 0.2) \times 10^4$. Both experimental slopes significantly differ from $d\Delta\rho/dN = (3.1 \pm 0.05) \times 10^4$ of curve 2 calculated with anisotropic n/N data. Curve 1 is parallelly shifted above the monolayer $\Delta\rho/N$ data. According to the predictions of the “heads-and-tails” model this shift might be due to the higher polarizability of the dry COOH groups in bulk crystals of RCOOH compared to the hydrated heads of the Langmuir monolayers ($\alpha_{COOH} = 3.3 \text{ \AA}^3$, $\alpha_{H_2O} = 1.5 \text{ \AA}^3$).

Mean Isotropic Refractive Indices of the LE, LS–S, and CS Phases. The mean isotropic refractive indices of the LS–S and CS phases were calculated from eq 4 (setting $n_z = n_x = n$) with the corresponding $\Delta\rho$ -values from Figure 5 and a monolayer thickness estimated from eq 11. To determine the thickness in the LE phase, we utilized its structural similarity with the lamellar liquid-crystalline phase.^{16,25} For the latter Larsson and Quinn²⁵ proposed a relationship

$$d_{L\alpha}/d_{Cr} = \sin\Phi \quad (12)$$

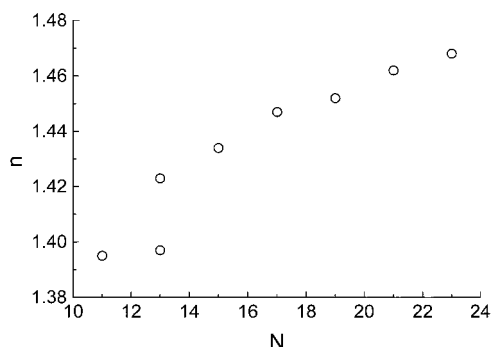


Figure 7. Mean isotropic refractive index of the fatty acid monolayers calculated with eqs 4 and 11 from the experimental $\Delta\rho/N$ data in Figure 5.

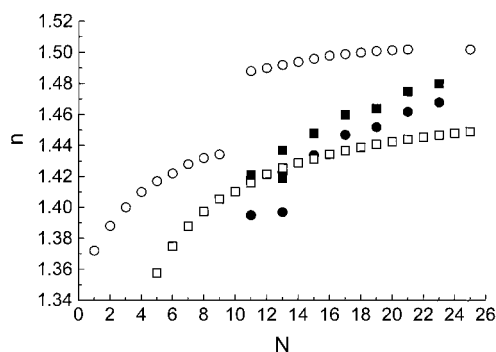


Figure 8. Comparison of the monolayer n/N dependencies calculated from eqs 4 and 11 with (full circles) and without (full squares) the heads included in the monolayer thickness. The open circles represent the bulk n/N data for liquid and solid fatty acids and the open squares the bulk dependence for the liquid and solid alkanes.

where $d_{L\alpha}$ is the lamella thickness in the L_α phase and d_{Cr} is the repeating thickness of the crystalline phase. $\Phi = 43^\circ$ denotes an effective statistical tilt angle of the disordered hydrocarbon chains toward the plane of the headgroups ($\Phi + \Theta = 90^\circ$). Identifying d_{LE} with $d_{L\alpha}$ and d_S with d_{Cr} and evaluating d_S from eq 11 we obtained the thickness of the lauric and myristic acid monolayers in the LE phase.

The mean isotropic refractive index thus obtained is plotted versus N in Figure 7. It can be seen that n of the fluid LE phase does not depend on the chain length. At the LE–LS transition in the myristic acid monolayer, where the area per molecule decreases from 27 to 19.2 \AA^2 , the refractive index of the monolayer increases jump wise. For the longer chains n varies monotonically with N . The jump of $\Delta\rho$ at the S–CS transition (see Figure 5) disappears here perhaps because the thickness of the S and CS phases was calculated with the same values of d_0 , d_{CH_2} , and d_{CH_3} , and the formation of a “staggered” structure was thus neglected.

Figure 8 shows the monolayer $n(N)$ dependencies calculated from the experimental $\Delta\rho/N$ data with full molecular length (full circles) and neglecting the contribution of the hydrophilic head to the monolayer thickness (full squares). They are compared with the bulk n/N data for the liquid and solid fatty acids (open circles) and liquid and solid alkanes (open squares). As can be seen there is no quantitative agreement between the monolayer and bulk n/N data. However, both the bulk and the monolayer n/N dependencies of the fatty acids exhibit discontinuities at the liquid–solid, respectively LE–LS phase transitions, while the bulk n/N dependence of the alkanes does not show such a change. At the same time the monolayer refractive indices are smaller than the bulk refractive indices of the solid fatty acids, as already reported by Hofmeister.⁵ This difference might be

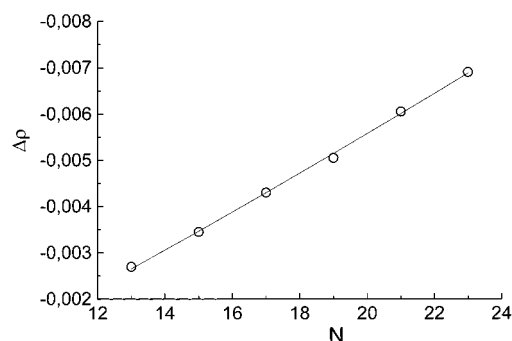


Figure 9. Fit of eqs 4, 7–10 of the “heads-and-tails” model to our experimental $\Delta\rho/N$ for the solid condensed monolayer state at $19.2 \pm 0.5 \text{ \AA}^2$. The fit performed at fixed $\alpha_0 = 2.5 \text{ \AA}^3$ and $d_0 = 6.5 \text{ \AA}$ gives $\alpha_{\perp,CH_2} = 1.83 \pm 0.02 \text{ \AA}^3$ and $\alpha_{\parallel,CH_2} = 1.84 \pm 0.06 \text{ \AA}^3$, which very well agrees with the independent value of $\alpha_{CH_2,istr} = 1.84$.

due to the higher polarizability of the dry carboxyl groups in the fatty acid crystals compared with the hydrated monolayer heads. This speculation is supported by the fact that the bulk and monolayer n/N dependencies of the fatty acids approach each other at high values of N , where the monolayer headgroups hydration and its relative contribution become smaller. At the same time the ellipsometric contribution of the COOH groups is clearly seen from the difference of the refractive index of the C25 alkane and acid.

Fit of the “Heads-and-Tails” Model to the $\Delta\rho/N$ Data. The fit of eqs 4 and 7–10 to the experimental $\Delta\rho/N$ data requires adjusting of five free parameters, Θ , α_0 , d_0 , α_{\parallel,CH_2} and α_{\perp,CH_2} , which is impossible for the limited number of experimental points. For this reason we consider only the solid condensed phases consisting of closely packed and vertically oriented chains with $\Theta = 0^\circ$ and analyze the $\Delta\rho/N$ dependence for the C14–C24 fatty acids at approximately constant area per molecule $F = 19.2 \pm 0.5 \text{ \AA}^2$. A further reduction of the number of the free parameters is achieved performing the fit at fixed values of α_0 and d_0 chosen according to the following physical restrictions: (i) The polarizability of the headgroups region α_0 should stay between the bulk water value 1.5 \AA^3 and the one of a dry carboxyl group 3.3 \AA^3 . The latter has been determined from the intercept of the linear plot of the molecular polarizability of fatty acids²⁶ versus the number of carbon atoms in the hydrocarbon chain. (ii) The thickness of the headgroups region d_0 should exceed the Z-dimension of a dry COOH group d_{COOH} (2.5 \AA from X-ray data¹⁸ and 3.9 \AA from the van der Waals volume²⁷) at a vertical molecular orientation. The upper limit of d_0 cannot be strictly specified, but it should be given by the sum of d_{COOH} and the thickness of the hydration shell, d_{H_2O} . Assuming that d_{H_2O} is close to the diameter of a H_2O molecule and taking the VdW value²⁷ of 2.8 \AA one comes to the limits $2.5 (3.9) \leq d_0 \leq 6.8 \text{ \AA}$. (iii) The previous investigations^{3,4,11,12} conclude that a solid condensed monolayer can be either isotropic or uniaxially anisotropic in Z-direction. Equations 7–10 show that a positive refractive index anisotropy ($n_z - n_x > 0$) means a positive anisotropy of the methyl group polarizability, $\alpha_{\parallel,CH_2} > \alpha_{\perp,CH_2}$. This requires $\alpha_{\parallel,CH_2} \geq \alpha_{\perp,CH_2} \approx \alpha_{CH_2,istr}$.

Figure 9 shows an example of a fit of our $\Delta\rho/N$ data at fixed $\alpha_0 = 2.5 \text{ \AA}^3$ and $d_0 = 6.5 \text{ \AA}$ satisfying the above criteria. The fit gives $\alpha_{\perp,CH_2} = 1.83 \pm 0.02 \text{ \AA}^3$ and $\alpha_{\parallel,CH_2} = 1.84 \pm 0.06 \text{ \AA}^3$, the two values coinciding within 3.3%. The values of $\alpha_{\parallel,CH_2} = \alpha_{\perp,CH_2}$ agree very well with $\alpha_{CH_2,istr} = 1.84 \text{ \AA}^3$, estimated from the slope of the linear chain length dependencies of the molecular polarizability of alkanes and fatty acids.²⁶

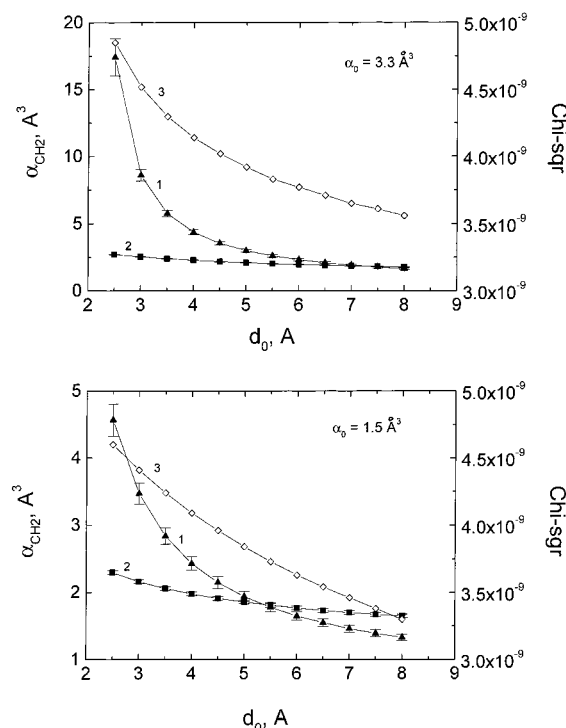


Figure 10. Dependencies of the anisotropic polarizabilities of the methylene group, $\alpha_{\parallel\text{CH}_2}$ (curve 1), $\alpha_{\perp\text{CH}_2}$ (curve 2), and the best-fit values of the χ^2 -criterion (curve 3) on the thickness of the headgroup region d_0 for the highest and lowest possible polarizability of the COOH-region, $\alpha_0 = 3.3 \text{ \AA}^3$ and 1.5 \AA^3 .

The fitting procedure illustrated in Figure 9 provides $\alpha_{\parallel\text{CH}_2}$ and $\alpha_{\perp\text{CH}_2}$ values for each couple of fixed α_0 and d_0 . These data are plotted versus d_0 in Figure 10 for the upper and lower limit of α_0 (note the different scaling of the ordinates). The variation of the best fit values of the χ^2 -criterion with d_0 is also presented. Similar dependencies were obtained for $\alpha_0 = 2.0$ and 2.5 \AA^3 confirming the following conclusions: (i) For a given value of α_0 the quality of the fit improves (the χ^2 value decreases) with increasing the headgroups dimension, d_0 , and decreasing anisotropy, $\alpha_{\parallel\text{CH}_2} - \alpha_{\perp\text{CH}_2}$. Therefore, according to the adopted restriction $\alpha_{\parallel\text{CH}_2} \geq \alpha_{\perp\text{CH}_2}$, the lowest χ^2 -value at a given α_0 corresponds to an isotropic monolayer. (ii) For all checked values of α_0 the isotropic polarizability of the methyl group $\alpha_{\parallel\text{CH}_2} = \alpha_{\perp\text{CH}_2}$ obtained from the fit very well coincides with the independently determined value $\alpha_{\text{CH}_2, \text{istr}} = 1.84 \text{ \AA}^3$. (iii) For the physical limits of $\alpha_0 = 1.5\text{--}3.3 \text{ \AA}^3$ the values of d_0 at which $\alpha_{\parallel\text{CH}_2}$ becomes equal to $\alpha_{\perp\text{CH}_2}$ (d_0 of an isotropic monolayer) fall between 5.4 ± 0.2 and $7.4 \pm 0.2 \text{ \AA}$. Both limits of d_0 exceed the X-ray (2.5 \AA) and van der Waals (3.9 \AA) dimension of a dry carboxyl group, thus implying that the monolayer heads in the solid condensed state are hydrated. Taking their average, $d_0 = 6.4 \text{ \AA}$, and the van der Waals values of $d_{\text{COOH}} = 3.9 \text{ \AA}$ and $d_{\text{H}_2\text{O}} = 2.8 \text{ \AA}$, one estimates that their hydration shell is approximately one (0.90 ± 0.35) water molecule thick.

The maximum anisotropy of the solid condensed fatty acid monolayer reported previously⁴ gives $\alpha_z/\alpha_x = 1.14$. Assuming that $\alpha_{\text{CH}_2, z}/\alpha_{\text{CH}_2, x} \approx \alpha_z/\alpha_x$ we find values of d_0 corresponding to this ratio from Figure 10 between 4.5 and 6.0 \AA for $\alpha_0 = 1.5\text{--}3.3 \text{ \AA}^3$. Both the low and the upper limits exceed the value of $d_{\text{COOH}} = 3.9 \text{ \AA}$, and their average suggests a hydration shell 0.50 ± 0.35 water molecules thick.

Kim et al.¹⁰ have shown that a 100% conversion of the fatty acid to $(\text{RCOO})_2\text{Pb}$ causes a significant shift to higher values

of $\delta\Delta$ without affecting the slope of the $\delta\Delta/N$ dependence. These authors mentioned different possible explanations as changes of the hydration water structure, penetration of water molecules into the monolayer, refractive index anisotropy. According to the predictions of the “heads-and-tails” model, a change of the anisotropy should alter also the slope of the $\delta\Delta/N$ dependence in contrast to the observation that it remained the same. We have fitted eqs 4 and 7–10 to the literature data of ref 10 recalculated in a $\Delta\rho/N$ scale and found the same behaviors as described above. The χ^2 -values decreased with decreasing of anisotropy giving a lowest value for the isotropic case if the restriction $\alpha_{\parallel\text{CH}_2} \geq \alpha_{\perp\text{CH}_2}$ is taken into account. The isotropic polarizability of the methylene group found from the fit agrees very well with the independent value of $\alpha_{\text{CH}_2, \text{istr}} = 1.84 \text{ \AA}^3$ also for this system. This result shows that the effect of the Pb^{2+} ions on the ellipsometric chain length dependence is not related to a change of monolayer anisotropy.

The fit of eqs 4 and 7–10 to these data did not converge at any reasonable values of d_0 if α_0 was less than 3.3 \AA^3 . Good fits with almost the same χ^2 -values were obtained for $\alpha_0 = 3.3\text{--}5.5 \text{ \AA}^3$ and $d_0 = 3.0\text{--}4.6 \text{ \AA}$; above the upper limits the fits also converged, but their χ^2 -values were higher. Unfortunately, no independent data about polarizability and dimensions of a dry $(\text{COO})_2\text{Pb}$ group could be found in the literature so that no additional physical limits could be set for this system. Nevertheless, relying on the limits of α_0 and d_0 obtained in this study and speculating with their mean values, $\bar{\alpha}_0 = 4.4 \text{ \AA}^3$ and $\bar{d}_0 = 3.8 \text{ \AA}$, one could conclude that the adsorption of Pb^{2+} ions increases the polarizability of the headgroups region above the one of the dry COOH ($\alpha_0 = 3.3 \text{ \AA}^3$) and decreases its thickness from $\bar{d}_0 = 6.4 \text{ \AA}$ for undissociated fatty acids to $\bar{d}_0 = 3.8 \text{ \AA}$ for the Pb-soaps. This decrease should be due to a (may be partial) dehydration of the headgroups which is in accordance with the lower solubility of the Pb-soaps in water compared with the solubility of the fatty acids.

The “isotropic” limits of α_0 and d_0 obtained from the fit of the “heads-and-tails” model to the $\Delta\rho/N$ data could be compared with the results of the X-ray reflectivity investigation of Kjaer et al.¹⁸ Plotting the dimensions of the carboxyl group obtained in ref 18 versus the area per molecule one obtains a good straight line whose extrapolation yields $d_0 = 2.5 \text{ \AA}$ at 18.5 \AA^2 and 5.0 \AA at 24 \AA^2 . The first molecular area is equal to the cross section of a hydrocarbon chain in a solid crystal and a CS monolayer phase and the second one corresponds to zero surface pressure and fully hydrated COOH. These values are considerably below the values found in this study. However, the deviation is in the same direction and has almost the same magnitude as the one observed by Wasserman et al.⁷ They found that the ellipsometric thickness of alkylsiloxane monolayers on silicone exceeded by 2.2 \AA the thickness determined from X-ray reflectivity measurements. This difference remains so far unclear and should be a matter of further investigations.

Conclusions

Continuous ellipsometric isotherms, $\Delta\rho/F$, of Langmuir fatty acid monolayers recording the coefficient of ellipticity at Brewster angle of beam incidence indicate most of the phase transitions found by X-ray reflectivity and diffraction investigations.

The chain length dependence $\Delta\rho/N$ extracted from the isotherms at the areas per molecule corresponding to the LE, LS or S, and CS phases ($F_{\text{LE}} = 28 \pm 1 \text{ \AA}^2$, $F_{\text{LS/S}} = 19.2 \pm 0.3 \text{ \AA}^2$, $F_{\text{CS}} = 18.5 \pm 0.3 \text{ \AA}^2$) clearly shows the LE–LS and S–CS phase transitions but does not distinguish the LS–S one.

The values of $\Delta\rho$ in the CS phase are higher than those expected from the extrapolation of the S-part of the $\Delta\rho/N$ dependence. This might be due to an effective increase of the monolayer thickness resulting from a "staggered" structure appearing at high surface pressure. The roughness of the monolayer–air interface produced by such an up and downward molecular rearrangement might also contribute to this effect.

Assuming a linearity of the LE part of the $\Delta\rho/N$ dependence one finds a zero intercept at $N = 0$ as indication of a negligible contribution of the hydrophilic heads to the ellipsometric signal for this monolayer state. The complete hydration of the carboxyl groups under such conditions makes this conclusion plausible.

The chain-length dependence of the mean isotropic refractive index of the monolayer, calculated from the experimental $\Delta\rho/N$ data and the "one-layer-model", does not quantitatively agree with the n/N data for liquid and solid fatty acids and alkanes in bulk. However, both the monolayer and bulk n/N dependencies of the fatty acids exhibit a discontinuity at the liquid–solid, respectively LE–LS, phase transitions, while the bulk n/N dependence of the alkanes does not show such a jump. This behavior demonstrates the significant contribution of the headgroups to the optical properties of the fatty acids both in bulk and monolayer state.

A two-layers "heads-and-tails" model is proposed to account for the above contribution. It relates the ellipsometric signal of the monolayer to the polarizability and thickness of the headgroup and hydrocarbon chain regions and to the optical anisotropy of the latter. Application of this model to our $\Delta\rho/N$ dependence for the solid condensed state ($F = 19.3 \pm 0.5 \text{ Å}^2$) shows that the anisotropy of the methyl group is below 3.3%. This conclusion is in accordance with the small anisotropy of the monolayer refractive index reported in the literature;^{3,4,12} the values of $(n_z - n_x)/n_z$ found for monolayers at the air–water interface and multilayers on solid substrates vary between 1.7 and 5.0%.

The Z-dimension of the headgroups in the isotropic solid condensed monolayer fall between 5.4 ± 0.2 and $7.4 \pm 0.2 \text{ Å}$ when their polarizability limits are taken. The mean value, $\bar{d}_0 = 6.4 \text{ Å}$, exceeds both the X-ray (2.5 Å) and the van der Waals (3.9 Å) dimension of a dry carboxyl group. This difference implies that the headgroups hydration shell in this monolayer state is approximately one water molecule thick.

If literature data⁴ for the anisotropy of the molecular polarizability are taken into account, one obtains lower limits for $d_0 = 4.5\text{--}6.0 \text{ Å}$ and a hydration shell about 0.5 molecules thick.

Application of the "heads-and-tails" model to the $\delta\Delta/N$ dependence of ref 10 explains the observation, that the addition

of Cd^{2+} and Pb^{2+} to the aqueous substrate parallelly shifts all data to higher $\delta\Delta$ -values. According to the model this effect is due to an increase of the polarizability and a decrease the thickness of the headgroup region (partial dehydration) resulting from counterion binding to the carboxyl groups.

Acknowledgment. The authors are sincerely indebted to Prof. David Beaglehole from the University of Wellington, New Zealand, for the useful suggestions in the development of the theoretical model and for the careful and critical reading of the manuscript.

References and Notes

- (1) Drude, P. *Annal. Phys. Chem.* **1891**, *43*, 126.
- (2) Beaglehole, D. In *Fluid Interfacial Phenomena*; Croxton, C. A., Ed.; Wiley: London, 1986; Chapter 11.
- (3) Ducharme, D.; Max, J.; Salesse, C.; Leblanc, R. M. *J. Phys. Chem.* **1990**, *94*, 1925.
- (4) Thoma, M.; Schwendler, M.; Baltes, H.; Helm, C. A.; Pfohl, T.; Riegler, H.; Moehwald, H. *Langmuir* **1996**, *12*, 1822.
- (5) Hofmeister, E. Z. *Phys.* **1953**, *136*, 137.
- (6) Allara, D. L.; Nuzzo, R. G. *Langmuir* **1985**, *1*, 45.
- (7) Wasserman, S. R.; Whitesides, G. M.; Tidswell, I. M.; Ocko, B. M.; Pershan, P. S.; Axe, J. D. *J. Am. Chem. Soc.* **1989**, *111*, 5852.
- (8) Ulman, A. *An Introduction to Ultrathin Organic Films*; Academic Press, Inc.: Boston, 1991; pp 3–4.
- (9) Engelsens, D. D.; De Koning, B. *J. Chem. Soc., Faraday Trans.* **1974**, *1*, 70.
- (10) Kim, M. W.; Sauer, B. B.; Yu, H.; Yazdaniyan, M.; Zografi, G. *Langmuir* **1990**, *6*, 236.
- (11) Paudler, M.; Ruths, J.; Riegler, H. *Langmuir* **1992**, *8*, 184.
- (12) Engelsens, D. D. *Surf. Sci.* **1976**, *56*, 272.
- (13) Petrov, J. G.; Kuleff, D.; Platikanov, D. *J. Colloid Interface Sci.* **1982**, *88*, 29.
- (14) Kobayashi, K.; Takaoka, K.; Ochiai, S. *Thin Solid Films* **1988**, *159*, 267.
- (15) Lundquist, M. *Chem. Ser.* **1971**, *1*, 197.
- (16) Knobler, Ch. M.; Desai, R. C. *Annu. Rev. Phys. Chem.* **1992**, *43*, 207.
- (17) Bibo, A. M.; Peterson, I. R. *Adv. Mater.* **1990**, *2*, 309.
- (18) Kjaer, K.; Als-Nielsen, J.; Helm, C. A.; Tippmann-Krayer, P.; Moehwald, H. *J. Phys. Chem.* **1989**, *93*, 3200.
- (19) Tippmann-Krayer, P.; Moehwald, H. *Langmuir* **1991**, *7*, 2303.
- (20) Schlossman, M. L.; Schwartz, D. K.; Pershan, P. S.; Kawamoto, E. H.; Kellog, G. J. Lee, S. *Phys. Rev. Lett.* **1991**, *66*, 1599.
- (21) Beaglehole, D. *Picometer Ellipsometer Operating Manual*; Beaglehole Instruments: Wellington, 1994.
- (22) Fang, J.; Wantke, K.-D.; Lunkenheimer, K. *J. Colloid Interface Sci.* **1996**, *182*, 31.
- (23) Gaines, G. Jr. *Insoluble Monolayers at Gas–Liquid Interfaces*; Interscience: New York, 1966; p 192.
- (24) Wolgast, S.; Foerster, G.; Brezesinski, G. In preparation.
- (25) Larssen, K.; Quinn, P. J. In *Handbook of Lipid Research*; Plenum Press: New York, 1996; Vol. 4, Chapter 8, p 417.
- (26) *CRC Handbook of Chemistry and Physics, 74th Ed.*; Lide, D. E., Ed. CRC Press: Boca Raton, 1993–1994; p 10–200.
- (27) Polymeropoulos, E. E. Private communication.